Carrier-mediated ferromagnetism in vanadium-doped $(Sb_{1-x}Bi_x)_2Te_3$ solid solutions

Zhenhua Zhou[a] and Ctirad Uher
Department of Physics, University of Michigan, Ann Arbor, Michigan 48109

Marek Zabcik and Petr Lostak
Faculty of Chemical Technology, University of Pardubice, 532 10 Pardubice, Czech Republic

(Received 27 January 2006; accepted 17 March 2006; published online 8 May 2006)

Ferromagnetism in tetradymite-type diluted magnetic semiconductors $(Sb_{1-x}Bi_x)_{1.98}V_{0.02}Te_3$ $(0 \leqslant x \leqslant 1)$ is revealed to be of hole-mediated nature. The increasing replacement of antimony with bismuth results in a monotonous decrease of the hole concentration and the Curie temperature while the electrical resistivity increases. The value of the Curie temperature shows a linear dependence of $Np^{1/3}$, where N is the vanadium concentration and p is the concentration of hole. This trend agrees with the mean-field theory predictions. © *2006 American Institute of Physics*.
[DOI: 10.1063/1.2200738]

Antimony telluride (Sb_2Te_3) and bismuth telluride (Bi_2Te_3) belong to the family of narrow-band-gap semiconductors $A_2^VB_3^{VI}$ (A=Bi, Sb and B=Te) with the tetradymite structure (space group D_{3d}^5).[1,2] As-grown single crystals of Sb_2Te_3 and Bi_2Te_3 typically have high carrier concentration of holes on the order of 10^{20} and 10^{19} cm^{-3}, respectively, due to the formation of native antisite defects.[3–6] Such high concentration of holes will have important influence on the magnetic and transport properties of Bi_2Te_3 and Sb_2Te_3 when they are doped with magnetic ions of the transition metal (TM) elements.

A couple of years ago, our group reported on the ferromagnetic order developing in vanadium-doped bulk single crystals $Sb_{2-x}V_xTe_3$ with $x \leqslant 0.03$.[7,8] It was found that such crystals support ferromagnetism to temperatures of up to 22 K. Ferromagnetic order was also observed in Cr-doped Sb_2Te_3.[9,10] Recently, we reported on a high Curie temperature of 177 K in an $Sb_{1.65}V_{0.35}Te_3$ thin film prepared by low temperature molecular beam epitaxy technique.[11,12] In bulk crystals of $Sb_{2-x}V_xTe_3$ the solubility of vanadium is severely limited and in this environment we did not detect any significant change in the free carrier density (holes) with the increasing content of vanadium. Yet, clearly, the Curie temperature was a strong function of the vanadium content, rising from about 11 K for x=0.01 to 22 K for x=0.03.[7] In thin films, where the concentration of vanadium is much larger, we have seen a rather strong dependence of the carrier density upon doping with vanadium. By varying the content of vanadium between x=0.15 and x=0.35, the concentration of holes at 300 K increased from 6.5×10^{20} to 1.6×10^{21} cm^{-3}. The high Curie temperature observed in thin films of $Sb_{2-x}V_xTe_3$ thus could be due either to a much higher concentration of vanadium ions or to a much larger density of holes, or both. It is not clear at this moment which one of the two effects influences ferromagnetism to a greater extent.

Sb_2Te_3 and Bi_2Te_3 form solid solutions $(Sb_{1-x}Bi_x)_2Te_3$ over the entire compositional range $0 \leqslant x \leqslant 1$.[13] This offers a convenient way of changing the carrier concentration and thus provides opportunities to investigate the influence of carrier concentration on the magnetic and transport properties in TM-doped diluted magnetic semiconductors $A_{2-x}^VTM_xB_3^{VI}$. In this letter we aim at studying the magnetic state of a series of $(Sb_{1-x}Bi_x)_{1.98}V_{0.02}Te_3$ alloys across a wide compositional range of x while keeping the nominal concentration of vanadium fixed at 0.02. In such compounds the dominant variable should be the carrier density as it decreases on going from the Sb-rich towards the Bi-rich structure.

Single crystals of nominal composition $(Sb_{1-x}Bi_x)_{1.98}V_{0.02}Te_3$ (x=0, 0.05, 0.25, 0.50, 0.75, and 1.0) were grown using the Bridgman technique starting with high purity Sb, Bi, V, and Te elements. Magnetization measurements with applied magnetic field parallel to the c axis (perpendicular to the cleavage plane) were made in a magnetic property measurement system (MPMS) equipped with a 5.5 T magnet. In-plane transport properties (electrical resistivity and Hall effect) were carried out with the aid of a low frequency (16 Hz) Linear Research ac bridge over the temperature range from 2 to 300 K. The actual sample composition was determined using electron microprobe analysis and is shown in Table I. The compositions were obtained by averaging 30 measurements at randomly selected points on the polished surface of each sample. Discrepancies between the nominal and actual contents of Bi are very small, less than 1 at. %. However, the discrepancies between the nominal and actual compositions of vanadium are relatively large. This is especially evident in samples with the Bi content $x \geqslant 0.5$. Thus, for x=0.5, only 0.22 at. % of vanadium can be incorporated while for $x \geqslant 0.75$, the actual vanadium concentration is less than 0.13 at. %, suggesting the solubility of vanadium in Bi_2Te_3 being very small. As was shown by Dyck *et al.*[7] and as we have already noted, vanadium concentration does not have an important influence on the concentration of holes within such low level of doping. Hence, one may attribute the change of carrier concentration in $(Sb_{1-x}Bi_x)_{1.98}V_{0.02}Te_3$ to the replacement of Sb with Bi.

Temperature dependent electrical resistivity ρ and Hall coefficient R_H (current perpendicular to the c axis and magnetic field parallel to the c axis) of $(Sb_{1-x}Bi_x)_{1.98}V_{0.02}Te_3$ are shown in Figs. 1(a) and 1(b). All samples show progressively increasing resistivity at temperatures above around 20 K,

[a]Electronic mail: zzh@umich.edu

TABLE I. Lists of the composition of $(Sb_{1-x}Bi_x)_{2-y}V_yTe_3$, vanadium concentration N, values of the resistivity ρ, Hall coefficient R_H, concentration of hole p at 300 K, Curie constant C, paramagnetic Curie temperature θ_{CW}, Curie temperature T_C, and diamagnetic contribution χ_0 from the matrix.

Nominal x (EPMA)	y (EPMA)	N (cm^{-3})	ρ ($\mu\Omega$ m)	R_H (cm^3/C)	p (cm^{-3})	C (emu K/mol Oe)	θ_{CW} (K)	T_C (K)	χ_0 (emu/mol Oe)
0 (0)	0.0168	1.052×10^{20}	6.64	0.0691	9.03×10^{19}	2.837×10^{-3}	17.0	17	-2.476×10^{-5}
0.05 (0.0477)	0.0199	1.241×10^{20}	7.91	0.0748	8.35×10^{19}	3.284×10^{-3}	16.5	16	-3.559×10^{-5}
0.25 (0.2468)	0.0171	1.048×10^{20}	15.23	0.1234	5.06×10^{19}	2.962×10^{-3}	12.0	14	-4.711×10^{-5}
0.50 (0.5006)	0.0110	6.603×10^{19}	18.68	0.2099	2.97×10^{19}	1.591×10^{-3}	7.2	6.5	-8.860×10^{-5}
0.75 (0.7437)	0.0066	3.891×10^{19}	21.64	0.3623	1.72×10^{19}	4.961×10^{-4}	5.6	6	-5.474×10^{-5}
1.00 (1.00)	0.0058	3.362×10^{19}	31.74	0.5858	1.07×10^{19}	2.876×10^{-4}	1.9	2	-8.602×10^{-5}

indicating degenerate semiconductor carrier transport behavior. As shown by the inset in Fig. 1(a), below a certain low temperature, the resistivity increases with the decreasing temperature and reaches a peak value before rapidly falling. Such a behavior is likely caused by spin-disorder scattering[14,15] and the sharp drop that follows is an indication of the transition to a ferromagnetic state. Magnetic measurements described in the following paragraphs verify this picture. As the concentration of Bi increases, the resistivity rises as a consequence of the decreasing carrier concentration. This is confirmed by the trend in the Hall effect shown in Fig. 1(b). The Hall effect is invariably positive and, assuming a single carrier model, the extracted density of holes at 300 K is presented in Table I. The sharp upturns in the Hall effect at very low temperatures are due to the ferromagnetic ordering which contributes in the form of an anomalous Hall effect. In the case of $Bi_{1.98}V_{0.02}Te_3$, the rising Hall coefficient upon decreasing temperature suggests a decreasing concentration of holes rather than a sign of the formation of ferromagnetism. Overall, on going from $Sb_{1.98}V_{0.02}Te_3$ to $Bi_{1.98}V_{0.02}Te_3$, the room temperature concentration of holes decreases by nearly an order of magnitude, from 9.03 $\times10^{19}$ to 1.07×10^{19} cm^{-3}. As already noted, crystals of Sb_2Te_3 have higher intrinsic concentration of holes than crystals of Bi_2Te_3. This is due to a greater density of antisite defects that are more prevalent in an environment of the smaller electronegativity difference and weaker bonding between Sb and Te as compared to bonding of Bi with Te.

Magnetic footprint of Bi substituting for Sb in the $(Sb_{1-x}Bi_x)_{1.98}V_{0.02}Te_3$ alloys is shown in Fig. 2 where magnetization is plotted as a function of temperature. All magnetization curves are virtually flat with a very small negative (diamagnetic) contribution until sharp upturns appear at low temperatures. The rapidly rising magnetization indicates increasing long range magnetic ordering as the temperature decreases. Apparently, the magnetic ordering temperature of $Sb_{1.98}V_{0.02}Te_3$ ($x=0$) is the highest and it decreases monotonously as x increases. Interestingly, the highest saturation magnetization is not observed in $Sb_{1.98}V_{0.02}Te_3$, i.e., the sample with the highest Curie temperature, but in a compound with $x=0.25$. This might be a result of changes in the band structure when a small amount of Bi is added to Sb_2Te_3 to form a solid solution. Studies on more dilute $(Sb_{1-x}Bi_x)_{1.98}V_{0.02}Te_3$ alloys with $0<x<0.25$ will be needed to clarify this issue.

The paramagnetic Curie temperature of the $(Sb_{1-x}Bi_x)_{1.98}V_{0.02}Te_3$ samples is determined from the fitting of the high temperature magnetic susceptibility data to the Curie-Weiss law of the form

$$\chi(T) = \frac{C}{T-\theta_{CW}} + \chi_0, \tag{1}$$

where C is the Curie constant, θ_{CW} is the paramagnetic Curie temperature, and χ_0 is the temperature independent contribu-

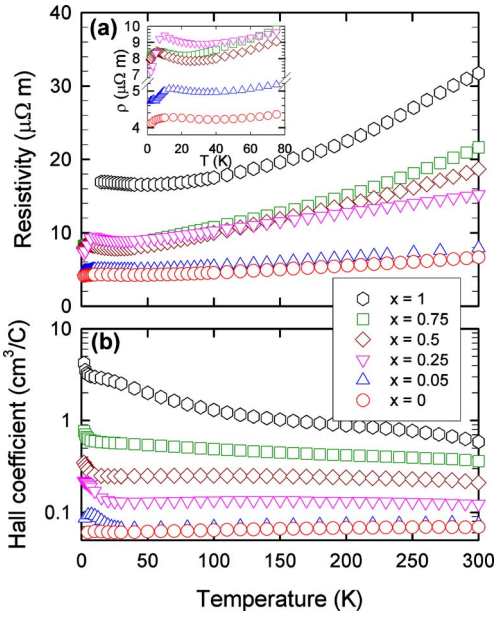

FIG. 1. (Color online) Temperature dependent (a) electrical resistivity and (b) Hall coefficient of $(Sb_{1-x}Bi_x)_{1.98}V_{0.02}Te_3$. The inset in (a) shows the low temperature behavior of resistivity.

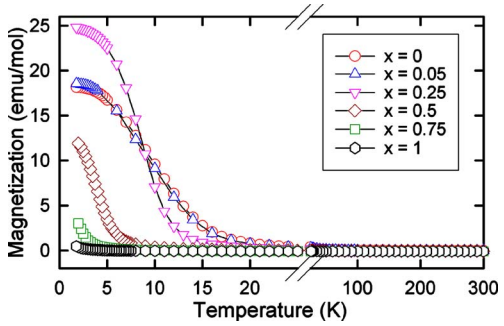

FIG. 2. (Color online) Magnetization of $(Sb_{1-x}Bi_x)_{1.98}V_{0.02}Te_3$ at an applied magnetic field of 1000 Oe parallel to the c axis.

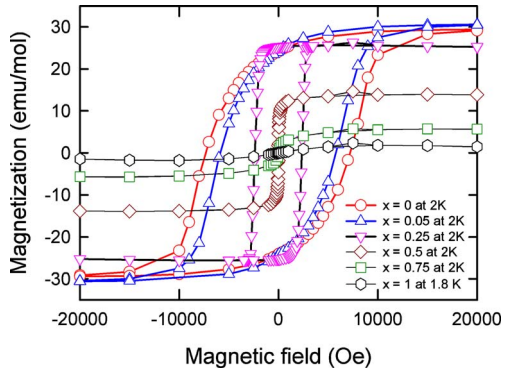

FIG. 3. (Color online) Magnetization vs applied field for $(Sb_{1-x}Bi_x)_{1.98}V_{0.02}Te_3$ with various contents of x measured at 2 K.

tion from the $(Sb_{1-x}Bi_x)_2Te_3$ matrix and the free carriers (holes in the present system). Fitting parameters are listed in Table I. Positive paramagnetic Curie temperatures θ_{CW} of 17.0, 16.5, 12.0, 7.2, 5.6, and 1.9 K are obtained for the samples with $x=0$, 0.05, 0.25, 0.50, 0.75, and 1.0, respectively. Clearly, the value of the paramagnetic Curie temperature decreases as the concentration of Bi increases. This indicates that the net ferromagnetic interactions in $(Sb_{1-x}Bi_x)_{1.98}V_{0.02}Te_3$ become weaker as the concentration of Bi increases. The Curie constant also decreases with the increasing concentration of Bi. Therefore, the replacement of Sb with Bi tends to weaken ferromagnetic interactions in the $(Sb_{1-x}Bi_x)_{1.98}V_{0.02}Te_3$ system. The Curie temperature T_C of the $(Sb_{1-x}Bi_x)_{1.98}V_{0.02}Te_3$ samples is pinpointed using Arrott plots since the effect of magnetic anisotropy and domain rotation is minimized in this approach. Arrott plots yield T_C of 17, 16, 14, 6.5, 6, and 2 K for the samples with $x=0$, 0.05, 0.25, 0.50, 0.75, and 1.0, respectively. These values are close with that of θ_{CW} determined from the Curie-Weiss analysis.

Figure 3 shows the magnetization versus applied field for $(Sb_{1-x}Bi_x)_{1.98}V_{0.02}Te_3$ at 2 K. Smooth hysteresis loops were obtained for all samples. As expected, the remanent magnetization and the coercive field decrease when the concentration of Bi increases, confirming the trend of the decreasing long range magnetic ordering upon replacement of Sb with Bi.

The Curie temperature T_C of $(Sb_{1-x}Bi_x)_{1.98}V_{0.02}Te_3$ samples depends strongly on both the vanadium concentration N and the hole concentration p. It indicates enhanced net ferromagnetic interactions at high concentrations of vanadium ions and charge carriers (holes). Figure 4(a) shows a plot of T_C as a function of $Np^{1/3}$ and a linear dependence is apparent. It is known that the Curie temperature of diluted magnetic semiconductors obtained from the mean-field theory has the following form[16]:

$$T_C \propto S(S+1)Nm^*p^{1/3}, \tag{2}$$

where S is the spin and m^* is the effective mass of the hole. This usually corresponds to the case of weak exchange coupling between the localized moments and the band carriers[17] when the concentrations of carriers and localized spins are relatively small. According to this formula, the increase of both vanadium concentration and hole concentration will result in an increase of T_C. Therefore, in order to further increase the Curie temperature, one will need to enhance the vanadium concentration and hole concentration substantially.

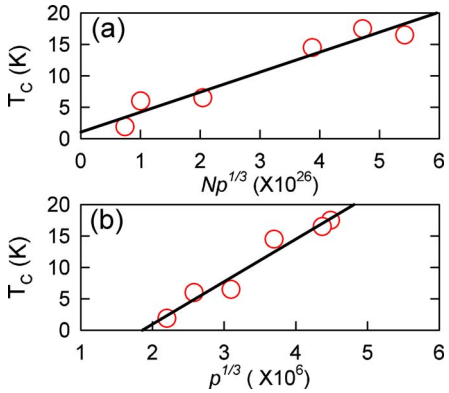

FIG. 4. (Color online) (a) Dependence of the Curie temperature T_C on $Np^{1/3}$ for $(Sb_{1-x}Bi_x)_{1.98}V_{0.02}Te_3$. (b) Dependence of the Curie temperature T_C on $p^{1/3}$ for $(Sb_{1-x}Bi_x)_{1.98}V_{0.02}Te_3$. N and p are in units of cm^{-3}.

This was confirmed by our thin film results.[11] Figure 4(b) shows a plot of T_C as a function of $p^{1/3}$. Linear dependence of T_C on $p^{1/3}$ strongly suggests that the observed ferromagnetism in $(Sb_{1-x}Bi_x)_{1.98}V_{0.02}Te_3$ is of hole-mediated nature.

In conclusion, we find that replacing Sb with Bi in $(Sb_{1-x}Bi_x)_{1.98}V_{0.02}Te_3$ results in a reduction of the ferromagnetic ordering temperature. This is due to a decrease in the carrier (hole) density as more and more Bi atoms substitute for Sb and undoubtedly also due to a reduction in the concentration of vanadium ions in the Bi-rich compounds where its solubility rapidly diminishes and it is not possible to keep vanadium concentration at or near the nominal value of 0.02. Clearly, the Curie temperature is a function of both the vanadium concentration and the hole concentration and its functional form agrees with the mean-field theory prediction.

This work was supported by the National Science Foundation Grants NSF-INT 0201114 and NSF-DMR 0305221, and by the Ministry of Education of the Czech Republic under the Project No. MSM 0021627501.

[1]T. L. Anderson and H. B. Krause, Acta Crystallogr., Sect. B: Struct. Crystallogr. Cryst. Chem. **B30**, 1307 (1974).
[2]D. L. Lovett, *Semimetals and Narrow-Band Gap Semiconductors* (Pion, London, 1977).
[3]S. Cho, Y. Kim, A. DiVenere, G. K. Wong, J. B. Ketterson, and J. R. Meyer, Appl. Phys. Lett. **75**, 1401 (1999).
[4]B. Roy, B. R. Chakraborty, R. Bhattacharya, and A. K. Dutta, Solid State Commun. **25**, 617 (1978).
[5]J. Horák, L. Tichý, P. Lošták, and A. Vaško, Cryst. Lattice Defects **6**, 233 (1976).
[6]Y. Kim, A. DiVenere, G. K. L. Wong, J. B. Ketterson, S. Cho, and J. R. Meyer, J. Appl. Phys. **91**, 715 (2002).
[7]J. S. Dyck, P. Hájek, P. Lošták, and C. Uher, Phys. Rev. B **65**, 115212 (2002).
[8]J. S. Dyck, W. Chen, P. Hájek, P. Lot'ák, and C. Uher, Physica B **312**, 820 (2002).
[9]J. S. Dyck, Č. Drašar, P. Lošták, and C. Uher, Phys. Rev. B **71**, 115214 (2005).
[10]V. A. Kulbachinskii, P. M. Tarasov, and E. Bruek, JETP Lett. **81**, 342 (2005).
[11]Z. Zhou, Y.-J. Chien, and C. Uher, Appl. Phys. Lett. **87**, 112503 (2005).
[12]Y.-J. Chien, Z. Zhou, and C. Uher, J. Cryst. Growth **283**, 309 (2005).
[13]H. J. Goldsmid, Br. J. Appl. Phys. **11**, 209 (1960).
[14]S. von Molnar and T. Kasuya, Phys. Rev. Lett. **21**, 1757 (1968).
[15]T. Kasuya, Prog. Theor. Phys. **16**, 45 (1956).
[16]C. H. Ziener, S. Glutsch, and F. Bechstedt, Phys. Rev. B **70**, 075205 (2004).
[17]J. Schliemann, J. König, H.-H. Lin, and A. H. MacDonald, Appl. Phys. Lett. **78**, 1550 (2001).